

Supporting Information

Demidenko et al. 10.1073/pnas.1002298107

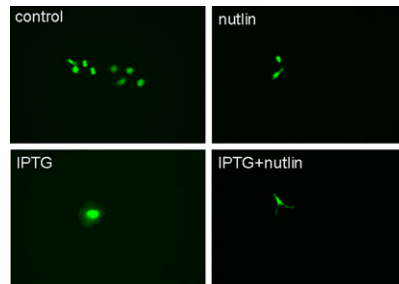


Fig. S1. Senescent versus quiescent morphology HT-p21 cells were treated with IPTG, nutlin-3a (10 μ M), and IPTG plus nutlin-3a for 3 days or left untreated (control). Live cells, visualized with GFP ($\times 100$). In control, cells underwent 3 divisions, forming a microcolony. IPTG-treated cells (large and flat) did not undergo any divisions. Nutlin-3a-treated cells were arrested after one division with normal cell morphology.

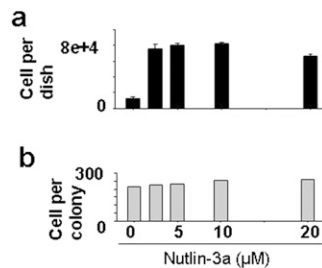


Fig. S2. HT-p21-9 cells were plated in 100-mm dishes and treated with IPTG in the presence or absence of nutlin-3a for 3 days. Then cells were washed and cultured for 9 days after drug removal. (A) Cell number per dish. Cells per dish were counted. (B) Cell number per a colony. Number of cells per colony was calculated. A number of cells per colony was 200–250 (approximately equal to eight divisions) by day 9. Thus, quiescent cells were characterized by normal proliferative potential after release from IPTG + nutlin-3a.

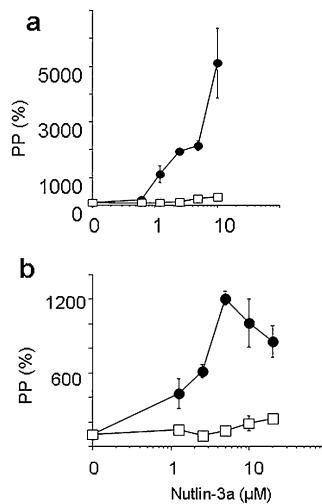


Fig. S3. Preservation of proliferative potential by Nutlin-3a. (A) Comparison of nutlin-3a and nutlin-3b in HT-p21-a cells. HT-p21-a cells were treated with IPTG in the presence of indicated concentrations of nutlin-3a (●) and nutlin-3b (□) for 6 days. Then medium was changed and cells were counted after 8 days. (B) Comparison of nutlin-3a and nutlin-3b in HT-p16 cells. HT-p16 cells were treated with IPTG in the presence of indicated concentrations of nutlin-3a (●) and nutlin-3b (□) for 3 days. Then medium was changed and cells were counted after 5 days.

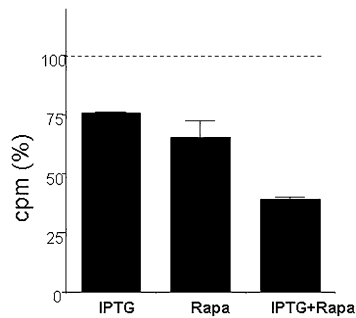


Fig. S4. Effects of IPTG and 500 nM rapamycin on protein synthesis ($[^{35}\text{S}]$ methionine/cysteine incorporation). Cells were treated as indicated for 24 h and then labeled with $[^{35}\text{S}]$ methionine/cysteine as described in *Methods*.

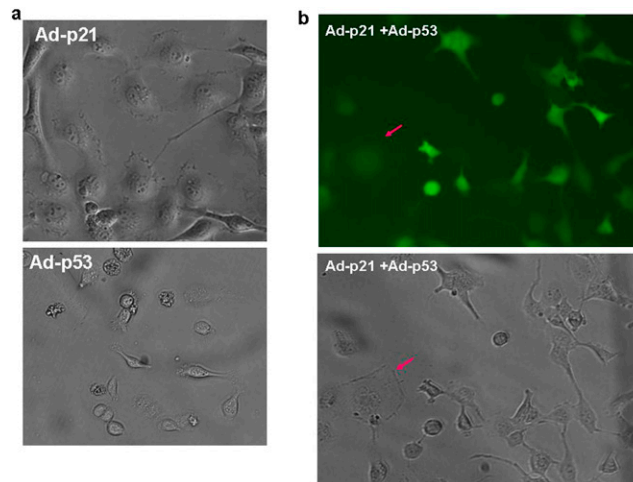


Fig. S5. (A) Effects of Ad-p21 and Ad-p53 on cellular morphology. p16-5 cells, derivatives of HT-1080 cells, were infected with either p21-expressing adenovirus (*Upper*: Ad-p21) or p53-expressing adenovirus (*Lower*: Ad-p53). Ad-p21 (*Upper*) caused large, flat cell morphology. Ad-p53 did not cause large, flat cell morphology. Cells were photographed at $\times 200$. (B) Ad-p53 suppresses senescent morphology caused by Ad-p21. p16-5 cells, derivatives of HT-1080 cells, were infected with Ad-p21 and Ad-p53. (*Upper*) Under blue light to visualize cells expressing p53 (green cells) ($\times 200$). (*Lower*) Under visible light to visualize all cells ($\times 200$). Red arrow is pointed at the cell with weak p53 expression. All other cells did not acquire large, flat cell morphology.

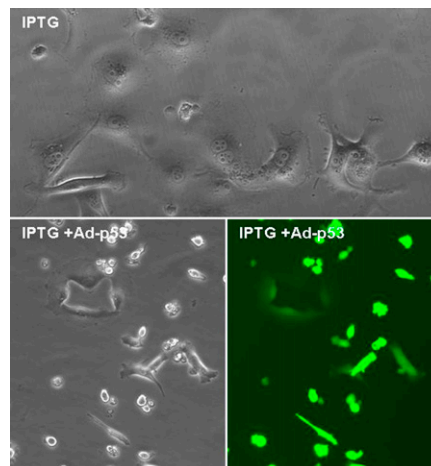


Fig. S6. Effects of Ad-p53 on senescent morphology caused by p16 p16-5 cells, derivatives of HT-1080 cells, were treated with IPTG (*Upper*) and IPTG plus Ad-p53 (*Lower*). IPTG (*Upper*) causes large, flat cell morphology. Ad-p53 prevents this morphology. Cells were photographed at visible light and blue light ($\times 200$) to visualize cells expressing p53.

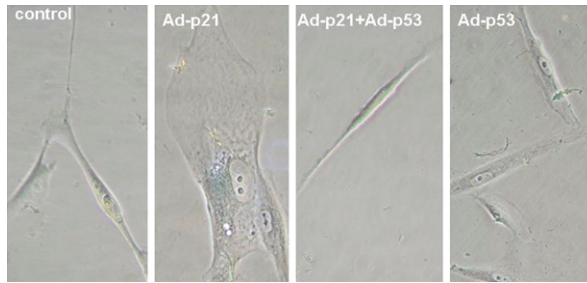


Fig. 57. Effects of Ad-p21 and Ad-p53 on senescent morphology in WI-38-tert fibroblasts. WI-38-tert cells were infected with either p21-expressing adenovirus (Ad-p21) or p53-expressing adenovirus (Ad-p53) or both. After 3 days, cells were stained for β -Gal.

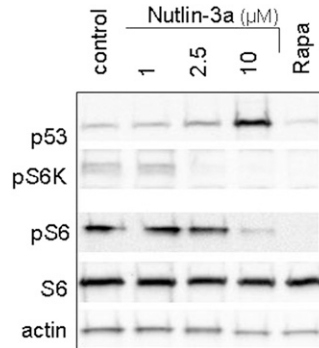


Fig. 58. Effects of nutlin-3a on p53 levels and S6/S6K phosphorylation in WI-38-tert fibroblasts. WI-38-tert cells were treated with indicated concentrations of nutlin-3a and 500 nM rapamycin (Rapa), as indicated, for 24 h. Immunoblot for p53, p-S6, p-S6K, S6, and actin was performed as described in *Methods*.

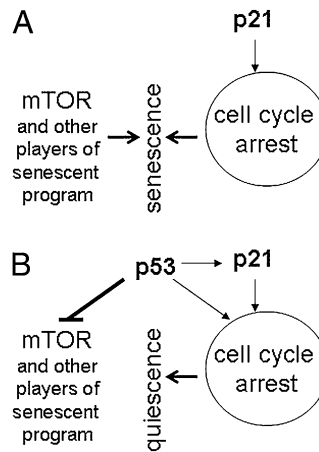


Fig. 59. Schema: Suppression of senescence by p53. (A) p21 causes cell cycle arrest, leading to senescence. (B) p53 causes cell cycle arrest and simultaneously inhibits the senescent program, leading to quiescence.